Electron–electron correlations in carbon nanotubes

Sander J. Tans*, Michel H. Devoret*†, Remco J. A. Groeneveld* & Cees Dekker*

** Department of Applied Physics and DIMES, Delft University of Technology, Lorentzweg 1, 2628 CJ Delft, The Netherlands*
† Service de Physique de l'Etat Condensé, CEA-Saclay, F-91191 Gif-sur-Yvette, France

Single-wall carbon nanotubes[1,2] are ideally suited for electron-transport experiments on single molecules because they have a very robust atomic and electronic structure and are sufficiently long to allow electrical connections to lithographically defined metallic electrodes. The electrical transport properties of single nanotubes[3] and bundles of nanotubes[4] have so far been interpreted by assuming that individual electrons within the nanotube do not interact, an approximation that is often well justified for artificial mesoscopic devices such as semiconductor quantum dots[5]. Here we present transport spectroscopy data on an individual carbon nanotube that cannot be explained by using independent-particle models and simple shell-filling schemes. For example, electrons entering the nanotube in a low magnetic field are observed to all have the same spin direction, indicating spin polarization of the nanotube. Furthermore, even when the number of electrons on the nanotube is fixed, we find that variation of an applied gate voltage can significantly change the electronic spectrum of the nanotube and can induce spin flips. The experimental observations point to significant electron–electron correlations. We explain our results phenomenologically using a model that assumes that the capacitance of the nanotube depends on its many-body quantum state.

Figure 1a shows an atomic force microscope (AFM) image of an individual metallic carbon nanotube, with a measured height of 1.4 nm, contacting two Al/Pt electrodes that are separated by 200 nm. The sample was fabricated as described elsewhere[3,6]. At room temperature the total resistance of the circuit is ~2 MΩ, with a contact resistance of the order of 500 kΩ. All presented measurements were performed in a dilution refrigerator with a mixing chamber base temperature of 5 mK. We apply a bias voltage (V_{bias}) to these electrodes and measure the d.c. current (I) through the nanotube. A third electrode at a distance of ~3 μm from the tube (outside the image) is used as the gate electrode to vary the electrostatic potential of the tube. Detailed transport spectroscopy measurements could be performed on this sample owing to its improved stability and reproducibility compared to our previous samples.

In Fig. 1b the differential conductance dI/dV_{bias} is displayed in colour as a function of V_{bias} and gate voltage (V_{gate}). The data reproduce many of the features found in previous electron transport experiments on metallic single-wall carbon nanotubes[3,4]. For example, when V_{gate} is swept at low V_{bias}, an almost periodic sequence of

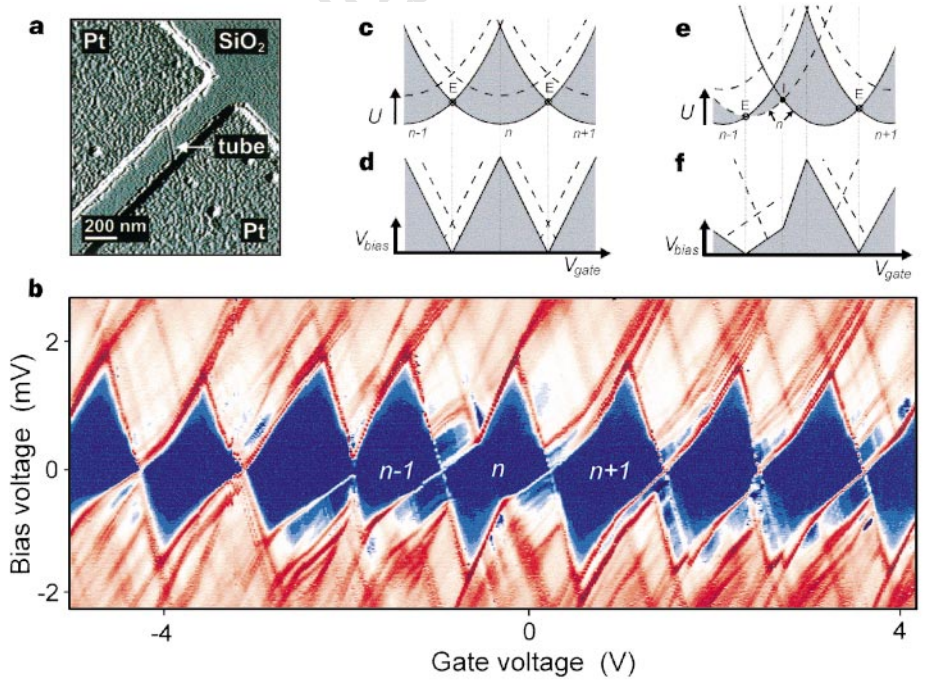

Figure 1 Transport spectrum of a single carbon nanotube at low temperature. **a**, AFM tapping-mode image of an individual carbon nanotube of 1.4 nm height, on top of a Si/SiO_2 substrate with electrodes of 25-nm-thick Al, capped with 5-nm Pt. A gate-electrode is positioned at a distance of 3 μm, outside the image. During the measurements, a minimum magnetic field B of 200 mT was applied perpendicular to the substrate in order to drive the Al from superconducting to normal. **b**, Differential conductance dI/dV_{bias} as a function of V_{bias} and V_{gate}: blue represents $dI/dV_{bias} = 0$, while red corresponds to a high dI/dV_{bias}. The data have been obtained by measuring many $I - V_{bias}$ curves for different V_{gate}. **c**, Energy diagram for a system with independent electrons. The energy U, equation (1), is plotted as a function of V_{gate} for ground states (solid lines) with $n - 1$, n, $n + 1$ excess electrons on the tube. Dashed parabolas represent excited states. Current can flow through the circuit when electrons can jump on and off the tube, that is, when transitions occur between parabolas of consecutive electron number (for example, n and $n + 1$). At low V_{bias} such an 'external' transition occurs at the points E. In between the two points E, the minimum V_{bias} for an external transition is proportional to the difference in energy between the two respective parabolas (grey area). **d**, Transition diagram in terms of V_{gate} and V_{bias} corresponding to **c**. The solid lines separate the coulomb blockade (CB) region where no current flows (grey) and the conduction regions where a current flows. Their slope is determined by the horizontal distance between the parabolas, which are equal here. **e**, Energy diagram when the excited-state parabola for n electrons is displaced with respect to the ground-state parabola. Now there is a discontinuity in the ground-state energy at point I, which marks an 'internal' transition between two states. **f**, Corresponding transition diagram which yields features in the CB region that are qualitatively similar to the experimental data of **b**.

sharp conductance peaks occurs, which is a signature of Coulomb blockade (CB) of the tube[7]. In the blue regions between these Coulomb peaks, no current can flow through the device because adding just a single electron will cost too much energy. In such a CB region, the system remains in its ground state with a fixed number n of excess electrons on the tube. At a Coulomb peak, transitions occur between ground-states of different electron number. At higher V_{bias} beyond the CB regions, additional lines are observed, signalling a stepwise increase of the current. The current steps result from transitions involving excited states that are well separated from the ground state. The energy spectrum of the tube thus is not continuous but discrete, as is expected for a tube of finite length.

We model the measured spectrum by considering the energy U of the system as a function of the external voltages V_{gate} and V_{bias} and the number of electrons n_r and n_l which have flowed through the right and the left junction, respectively. Assuming equal junction capacitances and symmetric voltage bias, the terms of the energy which are relevant here for a state with $n = n_r - n_l$ excess electrons on the tube are:

$$U = E_c\left(n - \frac{C_g V_{gate}}{e}\right)^2 - \frac{n_r + n_l}{2}V_{bias} + E_{kin} \qquad (1)$$

where $E_c = e^2/2C_\Sigma$ is the Coulomb energy for one additional electron. The symbols C_Σ, C_g denote respectively the total capacitance to the tube and the gate capacitance, and E_{kin} is the kinetic electronic energy of the state. As a function of V_{gate}, the energy U is a parabola. In Fig. 1c we schematically draw in solid lines the parabolas of three ground states with electron numbers $n-1$, n and $n+1$, which are equidistant. This diagram resembles a 'reaction coordinate diagram', which is often used to describe chemical reactions. In our case, the reaction coordinate V_{gate} is a voltage which is fixed externally. From this energy diagram one can deduce the conditions for current flow through the device by tracing possible transitions between parabolas of different electron number. The solid lines in Fig. 1d give these conditions for transitions, where electrons can jump on and off the nanotube, in terms of V_{bias} and V_{gate}. The grey area denotes the CB region, while the dashed lines represent excited-state transitions. Measurements on mesoscopic devices, such as semiconductor quantum dots and single-electron transistors, indeed yield such triangle-shaped CB regions[5].

When we compare the data of Fig. 1b with this model, striking deviations are observed. The transition lines in the data do not have identical slopes, even for a single CB region. Kinks and bends in the lines are frequent. The kinks in the CB region labelled n are particularly clear. Such a kink indicates that the system makes a transition to a different ground state. As the excess charge n at this transition does not change, we call it an 'internal' transition. For 'external' transitions, n does vary and current flows through the tube.

We propose a new model to explain these data qualitatively. We make the hypothesis that C_g is not solely dependent on the geometric shape of the nanotube and electrodes but can be a function of the many-body state adopted by the tube. This complication is unnecessary for larger artificial metallic structures[7] because external electric fields are perfectly screened inside the metal, leading to a state-independent capacitance. This last property is less and less verified as the dimensions of the structure become comparable to the screening length[8]. One may imagine that the electron densities of the one-particle wavefunctions have different spatial profiles. The various configurations of those states will therefore have varying capacitances. Another possibility is that electron–electron correlations make the effectiveness of screening dependent on the many-body state adopted by the tube. In our model, C_g thus depends both on n and on the degree of excitation of the tube, which induces a possible horizontal shift of the excited-state parabolas with respect to the corresponding ground-state parabolas. This is illustrated in Fig. 1e, which is similar to Fig. 1c, except that the two parabolas with the same electron number n are shifted with respect to each other. It leads to an internal transition at point I where a sharp discontinuity in the ground-state energy occurs. The corresponding transition diagram (Fig. 1f) now appears to have transition lines with different slopes and a kink at the discontinuity, which qualitatively resembles the data. The more complex multiple kinks or bends in other parts of Fig. 1b indicate that the complete spectrum is more complicated than in the diagram of Fig. 1f. More than two parabolas could be involved, and the position of the parabolas may be dependent on V_{bias}, which is not taken into account in this model.

In Fig. 2a we follow the position of the Coulomb peaks along the V_{gate}-axis as a function of magnetic field B between 0 T and 8 T. As the field is increased, the parabolas move up or down in energy depending on their spin due to the Zeeman effect, leading to shifts in the position of the Coulomb peaks (points E in Fig. 1e) along the V_{gate} axis. It has been shown that, in nanotubes, the Zeeman effect dominates the magnetic-field dependence and that orbital effects may be neglected[3,9]. This means that we can directly measure the spin direction of the incoming electron by the sign of the slope. From the average width of the Coulomb peaks at $V_{bias} = 100\,\mu V$ (data not shown), we can translate shifts along the V_{gate} axis to energy variations and obtain an average g-factor of 2 ± 0.5. The slopes dV_{gate}/dB of the different trace-sections in Fig. 3a appear to vary up to 25%. Such behaviour is expected in a model of shifted

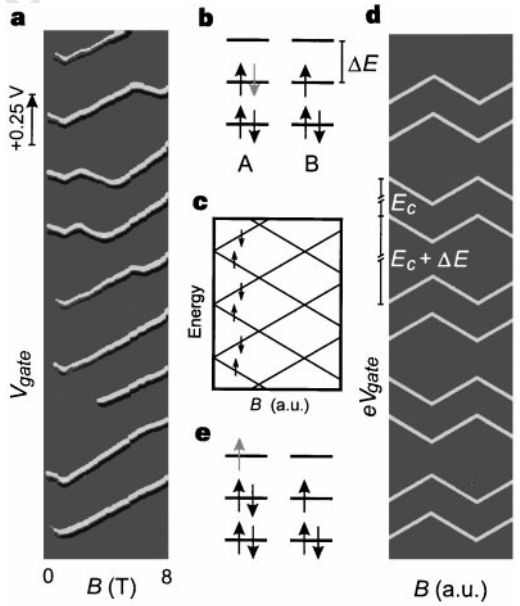

Figure 2 Evolution of the Coulomb peak positions as a function of the applied magnetic field, demonstrating spin-polarized states in the nanotubes. **a**, Numerical derivative dI/dV_{gate} is plotted in grey-scale as a function of V_{gate} and B, for $V_{bias} = 20\,\mu V$. The top trace is counted as the first trace and the bottom trace as the ninth trace. For clarity, all traces have been moved towards each other by an equal amount. The seventh peak has a very low intensity at low magnetic field, but is here seen to develop in a peak with normal intensity after 4 T. The shifts of the Coulomb peak positions are a result of the Zeeman effect. **b**, Two ladders of degenerate states (A and B) of the tube, with level separation ΔE. For an independent-particle filling scheme, similar configurations are found every four added electrons. After adding two 'up' spins, the next incoming electron (grey) must have a 'down' spin. **c**, Magnetic field evolution of the doubly degenerate levels corresponding to the filling indicated in **b**. **d**, Expectation for measurements corresponding to **c**: the traces would have an additional separation corresponding to the Coulomb energy E_c for each extra electron on the tube. The data show a different pattern of traces (**a**). From 0 to 1.3 T, the energy of all the visible transitions goes down in energy, indicating that the tube adopts non-trivial spin-polarized states. **e**, Possible filling scheme suggested by the data (**a**). The incoming electron (grey) that has spin 'up' must occupy a level with a higher kinetic energy.

parabolas (Fig. 1e, f) because the speed of the horizontal shift of point E now also depends on the horizontal distance between the parabolas.

The data indicate non-trivial shell-filling and spin polarization in carbon nanotubes. Nanotubes have a simple shell structure[10–12] with just two one-dimensional modes A and B. They are represented in Fig. 2b as two degenerate ladders of orbitals. Considering regular shell filling of independent particles, one would expect an up–down spin filling yielding a simple evolution of the states (Fig. 2c) and a corresponding movement of Coulomb-peak positions (Fig. 2d). In the data, we observe striking differences from this expected pattern. First, all the eight visible peaks appear to go down in energy from 0 T to ~1.3 T, which indicates that all electrons enter the tube with their spin parallel to the field. After 1.3 T, the peaks predominantly go up in energy. Second, adjacent traces do not show the expected correlation as indicated in Fig. 2d. Although paired lines are observed (for example, lines 3 and 4; see Fig. 2 legend for nomenclature), traces adjacent to this pair do not have kinks in opposite directions at the same magnetic field, which is a characteristic feature in quantum dots[5,13]. This implies that, at a given magnetic field, the $(n+1)$-electron ground state is not simply the n-electron ground state with one electron added in a new orbital.

In Fig. 3 we closely examine the second trace of Fig. 2a by plotting the numerical derivative dI/dV_{gate} of this peak at $V_{bias} = 500\ \mu V$ as a function of B. Because of the higher bias voltage, the trace has broadened into a stripe with additional structure due to excited-state transitions. Along the B-axis, the stripe consists of four segments, of which the second and the third appear to have clearly different widths in V_{gate}. This is very unusual for such measurements, and will be discussed below. As Fig. 2c shows, one expects levels to split from 0 T, which should also be observable in the excited-state spectrum as a line with a positive slope intersecting the lowest yellow line at 0 T in Fig. 3a. Such a feature is not observed in this Coulomb peak or in others. This lack of spin-splitting at 0 T reproduces our earlier results on an individual nanotube[3]. In contrast, transport studies in a bundle of nanotubes[9] have recently yielded the expected Zeeman splitting at 0 T. Our data also indicate that the patterns of excited-state transitions versus B (for example, Fig. 3a) are not correlated with the patterns of ground-state transitions (Fig. 2a), which is unexpected in a model of independent particle states.

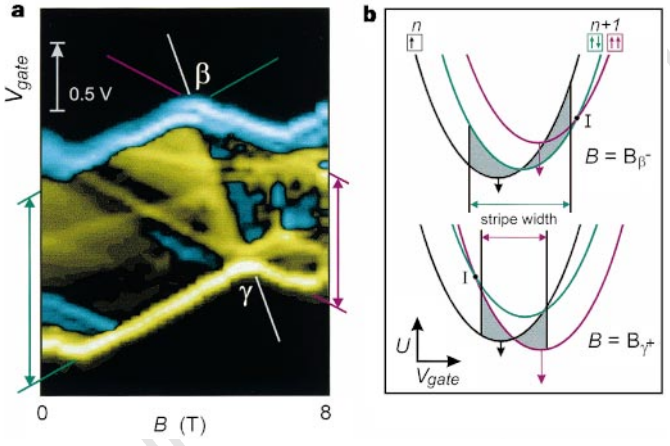

Figure 3 Evolution of the excited-state spectrum with magnetic field. **a**, Numerical derivative dI/dV_{gate} of trace 2 of Fig. 2a as a function of V_{gate} and B for $V_{bias} = 500\ \mu V$. Yellow lines correspond to transitions entering the bias window, while blue lines correspond to transitions leaving the window. The vertical widths in V_{gate} of the second (green) and the third (purple) segment are unequal. To model this unusual result qualitatively, we drawn in **b** a possible configuration of shifted parabolas just before kink β ($B = B_{β^-}$) and just after kink γ ($B = B_{γ^+}$). In **b** (top), the width of the second section of the stripe (green lines in **a**) is given by the horizontal width of the grey area, where transitions between the n-electron ground state with $m_s = 1/2$ (black parabola) and the $(n+1)$-electron ground state with $m_s = 0$ (green) can occur. The horizontal width of the grey area is determined by eV_{bias}, which is the maximum vertical distance between parabolas where transitions between the parabolas can occur. In going from β to γ, the parabolas shift with a speed indicated by the arrows. The triplet state moves twice as fast as the doublet, while the singlet state is unchanged. In **b** (bottom), the stripe is now narrower (purple lines in **a** and grey area for $B = B_{γ^+}$) because the $n+1$ ground state is now the purple parabola with $m_s = 1$, which is further away in V_{gate} from the black parabola than the green parabola. We note that the internal transition point I between the $n+1$ parabolas is shifted through the bias window from just to the right of the grey current area to just to the left with B. The line connecting β and γ in **a** traces this point I. In the traditional model (Fig. 1c), parabolas with the same n are positioned on top of each other, which yields a strictly vertical β–γ line. A non-vertical β–γ line signals a shift between parabolas associated with different spins.

We argue that the changing width of the stripe at the β–γ kink (Fig. 3a) is the consequence of an internal transition similar to the ones signalled by the kinks in the $V_{bias} - V_{gate}$ plot (Fig. 1b). The β–γ kink results from a crossing of two levels with different spins (see Fig. 3b). As the line connecting the two kinks β and γ is not vertical (which would lead to equal stripe widths), we know that the two corresponding parabolas are shifted with respect to each other. This in turn implies that at the crossing of the parabolas, an internal transition of a magnetic nature occurs. A curious situation thus occurs: changing the gate voltage results in a spin flip in the tube when the β–γ line is crossed. We suppose that such gate-voltage-driven internal magnetic transitions also exist down to $B = 0$. For example, we may extrapolate internal transition lines like the β–γ line to 0 T. In such a scenario, we can explain the fact that all the traces in Fig. 2a initially all go down with increasing magnetic field. Upon increasing gate voltage, we envisage a sequence for the total spin of the tube such as:

$$0 \rightarrow \frac{1}{2} \rightarrow 1 \rhd 0 \rightarrow \frac{1}{2} \rightarrow 1 \rhd 0 \rightarrow \ldots$$

where → marks an external transition increasing the number n of electrons by 1, and ▷ a magnetic internal transition where n stays constant. We note that at an external transition the spin is always increased, but between Coulomb peaks a hidden internal magnetic transition occurs which lowers the total spin of the tube. The spins of all incoming electrons can thus be parallel without having to invoke the existence of a gigantic spin polarization. This hypothesis implies that for certain gate voltage ranges, the ground state of the tube has a spin angular momentum higher than 1/2. In the simple sequence described above, the highest spin state would be a triplet state. Such a triplet state is shown in Fig. 2e where an incoming electron (grey) occupies an orbital with a higher kinetic energy. We now again consider the origin of the dependence of the capacitance on the quantum state of the nanotube and the resulting parabola displacement. We believe that a non-perfect and state-dependent screening due to electron–electron interactions is the cause of the parabola displacement, because models based on different spatial profiles of single-particle states do not produce the observed spin flips.

Thus, we have observed five features in the magnetic-field dependence of Coulomb peaks that cannot be explained by a simple shell-filling scheme of one-electron states. (1) At low fields, electrons always enter the nanotube with the same spin. (2) Kinks in adjacent traces of Coulomb peak position versus field do not occur at the same field. (3) The evolution of excited-state transitions with B is uncorrelated with the evolution of ground-state transitions with field. (4) Zeeman splitting at 0 T is not observed. (5) The gate voltage can induce spin flips. The first observation can be explained in a framework of one-electron states only if a very large exchange-type electron–electron correlation is present. For observations (2) to (5), however, a model based on one-electron states

does not suffice. These observations indicate that many-body states due to significant electron–electron correlations beyond exchange-type correlations have to be taken into account to describe the low-energy transport properties of carbon nanotubes. □

Received 5 February; accepted 11 June 1998.

1. Bethune, D. S. *et al.* Cobalt-catalysed growth of carbon nanotubes with single-atomic-layer walls. *Nature* **363,** 605–607 (1993).
2. Iijima, S. & Ishihashi, T. Single-shell carbon nanotubes of 1-nm diameter. *Nature* **363,** 603–605 (1993).
3. Tans, S. J. *et al.* Individual single-wall carbon nanotubes as quantum wires. *Nature* **386,** 474–477 (1997).
4. Bockrath, M. *et al.* Single-electron transport in ropes of carbon nanotubes. *Science* **275,** 1922–1925 (1997).
5. Sohn, L. L., Kouwenhoven, L. P. & Schön, G. (eds) *Mesoscopic Electron Transport* (Kluwer Academic, Dordrecht, 1997).
6. Thess, A. *et al.* Crystalline ropes of metallic carbon nanotubes. *Science* **273,** 483–487 (1996).
7. Grabert, H. & Devoret, M. H. (eds) *Single Charge Tunneling* (Plenum, New York, 1992).
8. Hallam, L. D., Weiss, J. & Maksym, P. A. Screening of the electron–electron interaction by gate electrodes in semiconductor quantum dots. *Phys. Rev. B* **53,** 1452–1462 (1996).
9. Cobden, D. H. *et al.* Spin splitting and even–odd effects in carbon nanotubes. *Phys. Rev. Lett.* **81,** 681–684 (1998).
10. Mintmire, J. W., Dunlap, B. I. & White, C. T. Are fullerene tubules metallic? *Phys. Rev. Lett.* **68,** 631–634 (1992).
11. Hamada, N., Sawada, A. & Oshiyama, A. New one-dimensional conductors: graphitic microtubules. *Phys. Rev. Lett.* **68,** 1579–1581 (1992).
12. Saito, R., Fujita, M., Dresselhaus, G. & Dresselhaus, M. S. Electronic structure of chiral graphene tubules. *Appl. Phys. Lett.* **60,** 2204–2206 (1992).
13. Tarucha, S., Austing, D. G., Honda, T., van der Hage, R. J. & Kouwenhoven, L. P. Shell filling and spin effects in a few electron quantum dot. *Phys. Rev. Lett.* **77,** 3613–3616 (1996).

Acknowledgements. We thank R. E. Smalley and co-workers for the supply of the indispensable single-walled carbon nanotubes. We also thank L. P. Kouwenhoven, T. H. Oosterkamp and Yu. V. Nazarov for discussions, and B. van den Enden for technical assistance. This work was supported by the Dutch Foundation for Fundamental Research on Matter (FOM).

Correspondence and requests for materials should be addressed to C.D. (e-mail: dekker@qt.tn.tudelft.nl).

Pairwise selection of guests in a cylindrical molecular capsule of nanometre dimensions

Thomas Heinz, Dmitry M. Rudkevich & Julius Rebek Jr

The Skaggs Institute for Chemical Biology and the Department of Chemistry, The Scripps Research Institute, 10550 North Torrey Pines Road, La Jolla, California 92037, USA

'Container' complexes in which a guest molecule is held mechanically within a cage-like host have been known for over a decade[1,2]. They provide a means to stabilize reactive intermediates[3] and to create new forms of stereoisomerism[4]. Molecular capsules held together by hydrogen bonds are more recent; they are formed reversibly on timescales of milliseconds to hours, long enough for molecular motions[5] and even reactions[6] to be seen for the encapsulated species. Here we describe the synthesis and characterization of a hydrogen-bonded molecular capsule of nanometre dimensions, which is large enough to encapsulate two different molecules. This allows us to explore the size- and shape-selectivity of the encapsulation process: we see, for example, the exclusive formation of the hetero-guest pair when benzene and *p*-xylene are both added to a solution. This presumably reflects optimal occupancy of the capsule—two benzene guests leave too much empty space in the interior, and two *p*-xylene molecules make it too crowded.

The synthesis of the new construct **1** (Fig. 1) uses methods developed by Cram[7] for the synthesis of velcrands (compounds whose molecules stick to one another) but leads to molecules of starkly different shapes and behaviours. Whereas the velcrands form dimeric structures through face-to-face aryl stacking interactions[7], compound **1** dimerizes through hydrogen bonding at its edges. The shape of **1** is vase-like, and the dimerization takes place in the rim-to-rim manner to give the large cylindrical capsule **1**·**1** (Fig. 1). It features dimensions ~1.0 × 1.8 nm and is stabilized by a 'seam' of eight bifurcated hydrogen bonds, with the imide hydrogens of one molecule directed between two carbonyl oxygens of another. This cyclic pattern of imides is, to our knowledge, without precedent.

The ^{1}H NMR spectra of **1**·**1** in $CDCl_3$, benzene-d_6 or toluene-d_8, show one sharp set of signals for all groups of protons (Fig. 2a, b and Fig. 3a), characteristic of C_{4v} symmetry of the subunits[8,9]. The spectra do not change within a 220–330 K temperature interval (toluene-d_8, $CDCl_3$), indicating high conformational stability. The NMR spectra in these solvents feature N-H signals far downfield at >9.5 p.p.m. and the Fourier-transform infrared spectrum of **1** in $CHCl_3$ shows only hydrogen-bonded N-H stretching absorption as a broad band at 3,332 cm^{-1} at > 0.3 mM concentrations.

Molecular modelling[10] suggested that two benzene or two toluene molecules could easily be accommodated inside the capsule, but the larger solvent mesitylene-d_{12} did not seem to fit well within the capsule. Some of the hydrogen bonds of the capsule become disrupted by the solvent, and indeed, multiple N-H signals were observed in the downfield region of the spectra in this solvent (Fig. 2c). This augured well for encapsulation studies in mesitylene-d_{12}, and the addition of suitable guests, such as bibenzyl, terphenyl, dicyclohexyl carbodiimide and *trans*-stilbene in that solvent restored the high symmetry of the capsule as reported by the NMR spectra (see for example, Fig. 4a). In addition, a second set of signals for the guest appeared, and their upfield shifts are characteristic of species encapsulated in aromatic containers[1]. The integration of the ^{1}H NMR spectra of these signals established the 1:1 stoichiometry of the host–guest assembly.

The encapsulation of less symmetrical guests such as *N*-phenyl benzylamine, benzyl phenyl ether, *trans*-4-stilbene methanol, and *p*-[*N*-(*p*-tolyl)]toluamide (Fig. 4b, c) shows the effect of molecular length on the rotational freedom of the guest and the overall symmetry of the complex. The NMR spectrum of the complexes shows a doubling of the capsule's signals: the two ends are different (Fig. 4b, c). These long guests can spin inside along the axis of the capsule, but are too large to 'tumble' within it. This restriction of motion is featured in the stereoisomerism discovered by Reinhoudt[4] in covalently bound carceplexes, and was also observed by Sherman[11] in reversibly formed capsules.

The capacity of **1**·**1** for small molecules—even common solvents—could also be directly observed in competition with mesitylene-d_{12}. In this solvent, the addition of (non-deuterated) toluene gave rise to a single set of sharp signals for the capsule in the NMR spectrum. Integration showed that two toluenes occupied the capsule (Fig. 4d). Toluene is small enough to tumble rapidly within the capsule on the NMR timescale at room temperature, and an averaged signal is observed for the methyl groups at −0.78 p.p.m.

The selectivity of the capsule was revealed through competition experiments involving two solvent guests. When both benzene and *p*-xylene were added in a 1:1 ratio (~30-fold excess) to the mesitylene-d_{12} solution of **1**, an asymmetrically filled capsule (see also Fig. 3b) was observed exclusively. One benzene (a singlet at 3.67 p.p.m.) and one xylene molecule (two aromatic doublets at 5.48 and 3.08 p.p.m.; $J = 6.3$ Hz, and one of two methyl singlets at −2.81 p.p.m.; another one is hidden) were found encapsulated. Apparently, the capsule with two xylene molecules is too crowded; both modelling[10] and ^{1}H NMR spectroscopy suggested that two xylenes cannot easily fit inside. Instead, a comfortable occupancy is reached with one of each guest in the capsule (Fig. 3b). The complex is asymmetrical because the two guests cannot squeeze past each other to exchange positions in the capsule—at least not on the NMR timescale. Likewise, benzene paired with *p*-trifluoromethyltoluene, *p*-chlorotoluene, 2,5-lutidine and *p*-methylbenzyl alcohol (Fig. 3c) to give species with one of each guest inside. The chemical shift of